Open File Report OF85-4

Platinum–Palladium Distribution in Ultramafic Rocks of the Bird River Complex, Southeastern Manitoba

By P. Theyer

Manitoba
Energy and Mines
Geological Services

1985

CONTRIBUTION TO PROGRAMMING CONDUCTED UNDER THE CANADA-MANITOBA INTERIM AND MINERAL DEVELOPMENT AGREEMENTS

Manitoba
Energy and Mines
Geological Services

Open File Report OF85-4

Platinum-Palladium Distribution in Ultramafic Rocks of the Bird River Complex, Southeastern Manitoba

By P. Theyer

Winnipeg, 1985

Energy and Mines

Hon. Wilson D. Parasiuk
Minister

Charles Kang
Deputy Minister

Geological Services
W. David McRitchie
Director

TABLE OF CONTENTS

APPENDICES

TABLE

FIGURES

ABSTRACT

The ultramafic portion of the Bird River Complex (BRC) is composed of at least thirteen igneous units characterized by cyclically repeated unidirectional developments of olivine crystal habits. It has been shown that crystal morphologies are sensitive to the environment of crystallization (Drever and Johnston, 1957) and that olivine crystal shapes are mainly dependent on the melt's degree of supersaturation (Donaldson, 1974; Lofgren and Donaldson, 1975). Donaldson (1976) demonstrated that the morphological complexity of olivine crystals in a melt is mainly a function of the cooling rate. It is thus proposed that the cyclically repeated increase of the complexity of crystal shapes observed from the stratigraphic bottom to the top of the igneous cyclic units in the BRC is caused by differences in the cooling rate, i.e., relatively rapid cooling at the top, becoming progressively slower with increasing depth.

Pt and Pd concentrations vary between each cyclic unit and correlate with abundances of S, Cu and Ni. Chromite is generally not associated with Pt and Pd; however, an exception is observed in cycle 10 of the eastern cut. Significant inhomogeneities in lateral distribution of Pt and Pd within a rock layer are suggested by the observation of high concentrations (179 ppb Pt, 532 ppb Pd) in a distinctive sulphides and chromite rich layer in the western cut. Even higher concentrations (511 ppb Pt, 1145 ppb Pd) were recorded in samples taken from this layer but approximately 50 m east of the western cut.

It is suggested that the ultramafic portion of the BRC may not be a simple intrusive body, but a multilayered igneous complex that contains significant amounts of Pt and Pd.

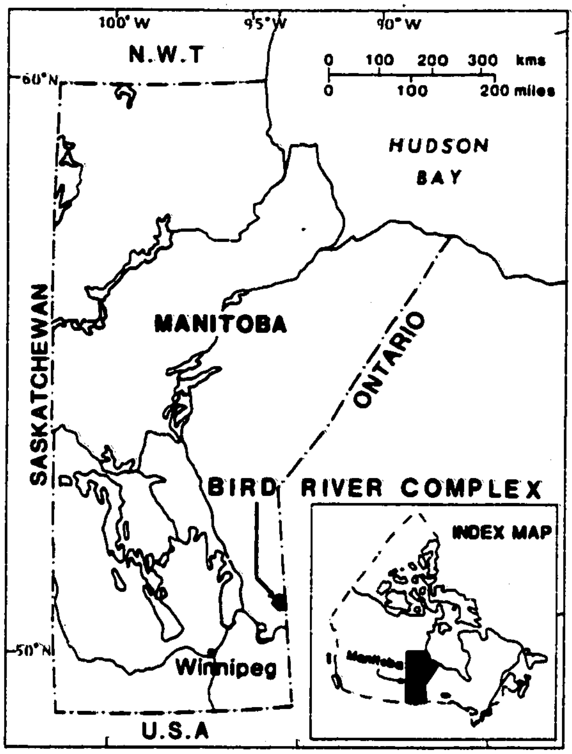

Figure 1: Location of the Bird River Complex, Manitoba, Canada. After Talkington et al., (1983) with modifications.

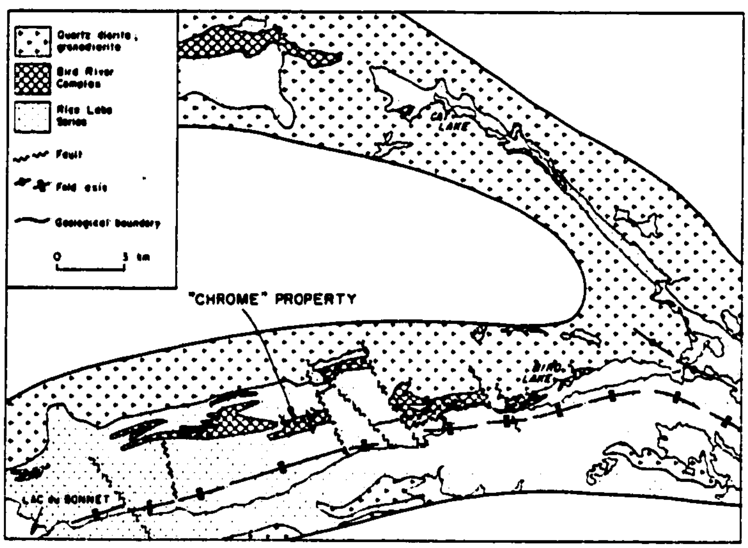

Figure 2: General geology of the Bird River Complex and location of the "Chrome" property. After Trueman (1971) with modifications.

INTRODUCTION

Platinum group elements (PGE) are concentrated in some stratiform ultramafic to mafic rock complexes in stable Archean cratons. Recent improvements in assaying techniques and analytical detection limits (Haffty et al., 1977; Hoffmann et al., 1978), combined with a steady demand and relatively stable prices have resulted in a surge of interest in these commodities.

The Bird River Complex (BRC) is a stratiform mafic to ultramafic rock assemblage of Archean age (Timmins et al., 1985). This paper presents the results of a study initiated in 1982 that investigated the distribution of Pt and Pd in the BRC.

LOCATION AND GENERAL GEOLOGY

The BRC in southeastern Manitoba, Canada (Fig. 1) is a stratiform mafic to ultramafic rock complex that occurs in the north and south limbs of an east plunging anticline (Fig. 2) in the Rice Lake Group of volcanic and sedimentary rocks (Trueman, 1971). In the area of the Chrome property (Fig. 3) which is located on the south limb of the anticline, the BRC is subdivided into a northern, stratigraphically lower ultramafic zone that is overlain by a southern mainly gabbroic rock suite (Trueman, 1971). Rocks of the BRC are weakly deformed and metamorphosed to the lower amphibolite facies (Ermanovics and Froese, 1978; Coats et al., 1979).

PREVIOUS WORK

Initially, interest in the geology and mineral potential of this area was generated by the discovery of Ni and Cu sulphides near the northern limb of the BRC in 1917 (Colony, 1920; Cooke, 1922; Wright, 1932). Chromite-bearing rocks discovered in 1941 were considered to be part of a faulted, but originally continuous sill (Bateman, 1943). Subsequent investigations by Springer (1948, 1949, 1950), Davies (1952) and Trueman (1971) are summarized in Trueman (1980). Bateman (1943) envisaged the BRC to have formed as a result of two different magmatic pulses: the first of ultramafic composition, followed by a separate pulse of mafic (gabbroic) composition. Osborne (1949)

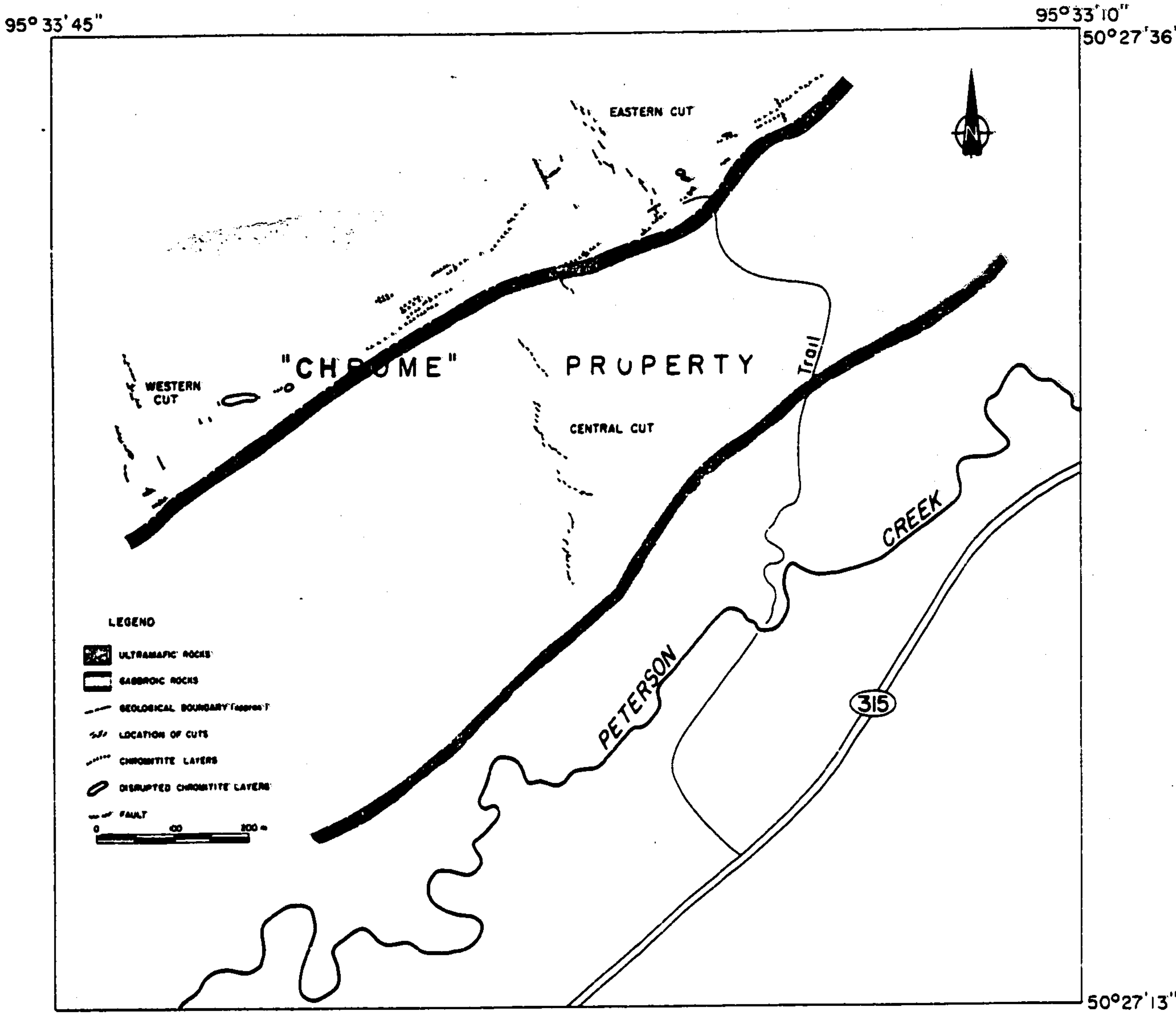

Figure 3: Schematic geology of the "Chrome" property and location of sawn samples (cuts).

proposed a complex multi-injection model, whereas Trueman (1971) and Scoates (1983) favored a single magmatic injection followed by in situ differentiation.

INVESTIGATION TECHNIQUES

Three semi-continuous sampling sections were cut across the BRC using portable rock saws. The western and the eastern "cuts" were sawn across the ultramafic portion of the BRC, whereas the central cut was sawn across a large part of the gabbroic unit (Fig. 3). These cuts provided an approximately continuous sampling across the steeply dipping rocks. Despite the lack of continuous exposures, the cutting of numerous short sections (Fig. 3) resulted in a semi-continuous cross-section with only minor overlaps and gaps. The position and length of all gaps are recorded on the tables and graphs.

Petrographic studies were conducted on more than 200 thin sections and over 600 polished rock slabs. Concentrations of S, Cu, Ni, Au, Pt and Pd were determined for approximately 250 samples. Selected samples of the eastern cut were also analyzed for Cr and several samples were analyzed for Os, Rh, Ru and Ir. Sample intervals were initially 2 m, however, this was reduced to 50 cm for follow-up work.

Chemical laboratories, analytical techniques, detection levels and computational conventions used are given in the data tables.

PETROGRAPHY

Ultramafic rocks of the BRC consist predominantly of serpentines after olivine. Olivine has also been replaced by chlorite and tremolitic amphibole. Other minerals present are diopsidic clinopyroxene, in places amphibolitized and/or chloritized, magnetite, chromite, minor talc and carbonate. Chromite, normally an accessory mineral, occurs as chromitite layers within the upper part of the ultramafic section of the BRC. These layers have been investigated for their economic potential and a summary of investigations was recently published by Bannatyne and Trueman (1982) and Watson (1985).

The original textures of the rocks are excellently preserved despite serpentinization (Fig. 5). The intercrystalline matrix composed of very fine grained acicular and plumose mineral aggregates (chlorite?) is interpreted to have been devitrified glass.

IGNEOUS CYCLES

Crystal habits have received widespread attention from petrologists since crystal shapes are sensitive to their environment of crystallization. Drever and Johnston (1957) presented an excellent summary of their own and previous research on crystal habits of forsteritic olivine and concluded that skeletal olivine crystals indicate rapid *in situ* crystal growth in an undercooled magma. More recent experimental evidence indicates that skeletal crystal growth can be induced in a supersaturated magma (Lofgren and Donaldson, 1975) and that supersaturation in a magma is generally caused by supercooling, but to a minor extent may also be caused by rapid decay of confining pressure and/or rapid loss of volatiles (Donaldson, 1974). Donaldson (1976) also established that the morphological complexity of olivine crystal shapes in a melt is mainly a function of its cooling rate. He also argued that skeletal crystal habits of olivine are the result of crystal growth rather than crystal resorption; a concept that had been previously supported by Drever and Johnston (1957) and by Martin and MacLean (1973).

Olivine crystals in the BRC exhibit repeated progressions from simple, ovoid crystal habits to complex dendritic crystals with several intermediate stages of increasing crystal complexity. The stratigraphic base of an idealized magmatic cycle (Fig. 4) is defined as a layer of fine grained, tightly packed granular olivine cumulate (lensoid stage) that has an abrupt lower contact with skeletal (hopper) or dendritic olivine. This type of contact is shown in Figure 5B drawn from a polished rock slab of the eastern cut. However, in most cases the beginning of a new magmatic cycle is indicated by an abrupt reversal of the normal crystal habit development sequence.

The textural stages in the idealized magmatic cycle (Fig. 4) are:

1. Lensoid stage: This textural stage is characterized by oval to subrounded, small (1.6 mm average long axis) tightly packed olivine crystals that form a crystal supported cumulate (Fig. 4, stage 1). The groundmass consists mainly of devitrified glass. This stage ranges from a few cm to approximately 2 m in thickness.

2. Porphyritic stage: An initially subtle but eventually rapid decrease of crystal packing density results in a matrix supported fabric, concurrent with a marked growth in the size of individual olivine to 2 - 3 mm with crystal habits, similar to those in the lensoid stage, is called the porphyritic stage (Fig. 4, stage 2; Parts of Fig. 5A and upper part of Fig. 5B). The thickness of this stage ranges from a few cm to approximately 1 m.

3. Rod Stage: This stage is characterized by olivine crystals exhibiting a pronounced elongation of one crystal axis. A common length to width ratio is approximately 5:1. The individual crystals are matrix supported and are well separated from each other by a groundmass consisting mainly of devitrified glass. The rod stage ranges from a few cm to approximately 1 m in thickness. (Fig. 4, stage 3)

4. Rods with buds stage: Olivine crystals in this stage occur basically in the rod stage configuration, however, they are characterized by

the occurrence of minute buds that mar the normally smooth rod shaped crystal surfaces. The transition of the rod stage to the rod with buds stage is gradual. (Fig. 4, stage 4)

5. Horseshoe stage: Olivine crystals of the horseshoe stage are rod shaped olivine crystals that exhibit a pronounced curvature of their long axis resulting in the "U" shaped olivine crystals. This crystal habit stage ranges between 1 m and several metres in thickness. (Fig. 4, stage 5)

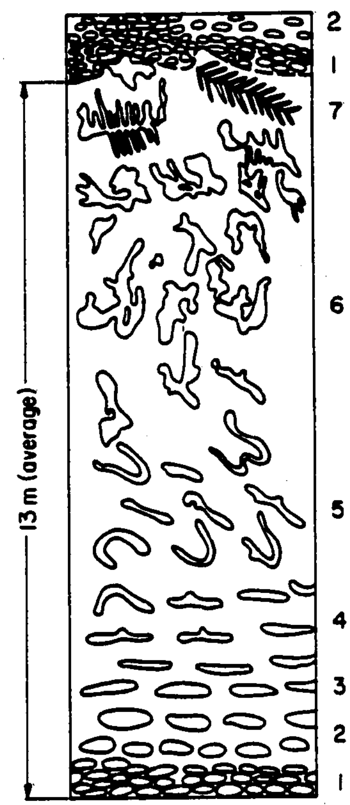

Figure 4: Stratigraphy of an idealized cyclic magmatic unit. Textural stages of olivine crystals: 1. Lensoid stage. 2. Porphyritic stage. 3. Rod stage. 4. Rods with buds stage. 5. Horseshoe stage. 6 Hopper stage. 7. Dendritic olivine.

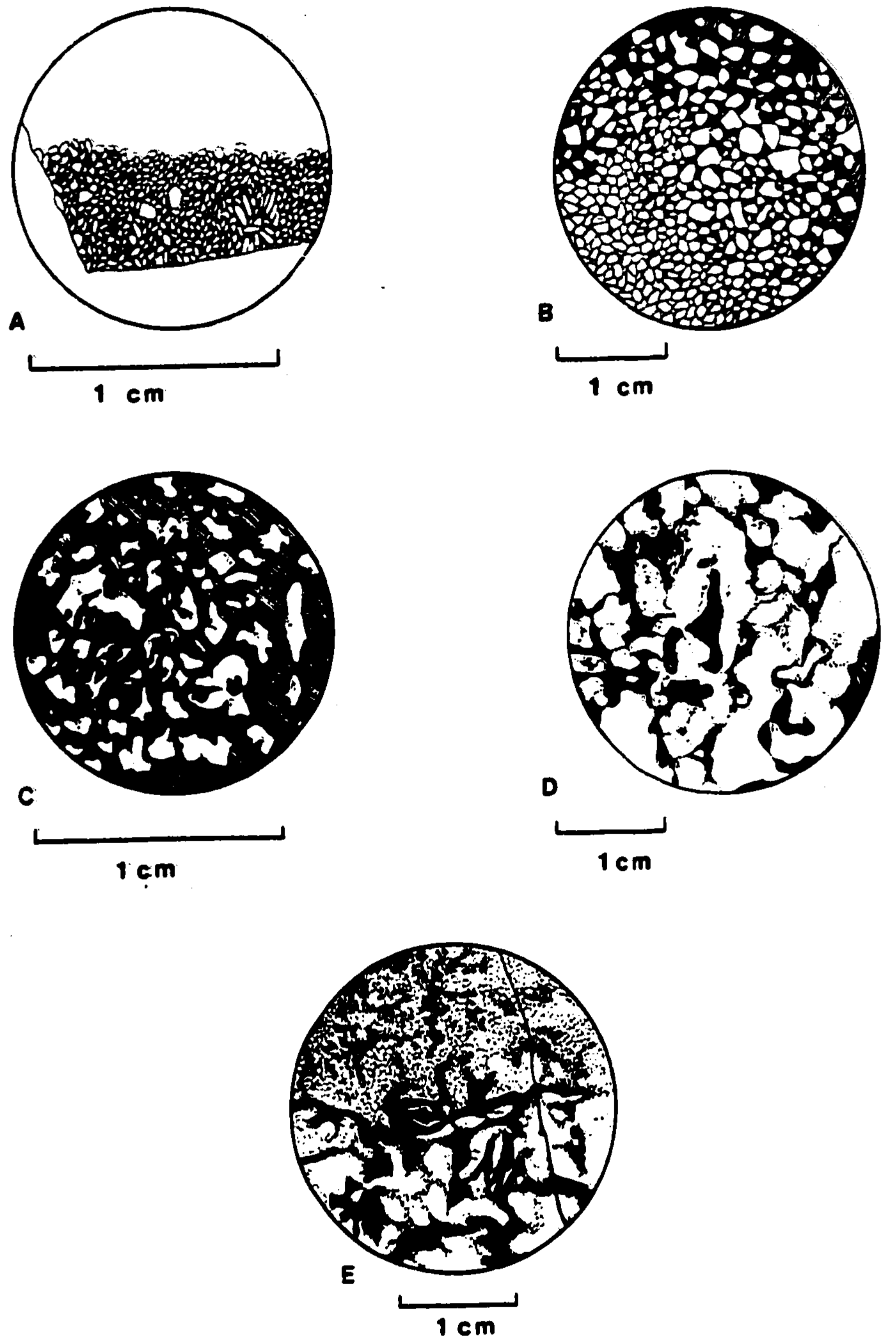

Figure 5: Textures of polished rock slabs. A. Olivine crystals of the lensoid stage, but several zones show a decrease of crystal packing density to the porphyritic stage. B. Transition from lensoid stage (lower part) to porphyritic stage (upper part). C. Hopper stage (small crystals). D. Hopper stage (large crystals). E. Contact between two cyclic units; overlying the hopper stage olivine of the lower cycle, are tightly packed lensoid stage olivines of the stratigraphically higher cycle.

6. Hopper stage: Olivine crystals of this stage are characterized by bumpy, subrounded amoeboidal shapes with numerous embayments. Crystal sizes range from a few mm to 3 cm. Most of the crystal shapes of this stage are interpreted as the basic "U" shaped horseshoe stage crystal, adorned by numerous buds and branches. (Fig. 4, stage 6; Fig. 5, C and D.) The hopper stage is by far the predominant texture in the BRC. Rock layers characterized by hopper olivine range between 1 m and 30 m thickness. The term "hopper" olivine for this crystal shape was first used by Donaldson (1976).

7. Dendritic olivine: These olivine crystals grow as wispy dendritic aggregates out of a common stem resulting in fern shaped crystals up to 10 cm long. This type of olivine crystal was observed in only one, approximately 30 cm thick, rock layer of the eastern cut.

On the basis of crystal morphologies, the ultramafic part of the BRC is subdivided into thirteen cycles in the western cut (Fig. 6) and thirteen cycles in the eastern cut (Fig. 7). The cycles range from 1.5 m to 46 m and average approximately 13 m in thickness. Most cycles contain several parts of the idealized crystal habit sequence shown in Figure 4; however, others are missing either because they are very thin layers or have been truncated by structural dislocations.

The rock textures and crystal habits within two of these magmatic cycles (cycles 5 and 6 of the western cut, Fig. 6) are described for illustrative purposes. Cycle 5 (from approximately 52.5 m to approximately 62.2 m) is characterized at its stratigraphic bottom by an approximately 15 cm thick layer of lensoid stage olivine. Olivine crystals are rounded to oval measuring an average of 0.28 mm in diameter and are in a tight packing with little or no intercrystalline matrix. An increase of crystal sizes (up to approximately 1 mm average diameter) concurrent with a pronounced decrease of the crystal packing density (ratio of crystals to groundmass approximately 80:20) over a few centimetres leads to the porphyritic stage. Stratigraphically higher parts of the porphyritic stage include a few randomly distributed rod-shaped and horseshoe-shaped olivine crystals; however, within this particular cycle the rod stages and the horseshoe stage are not well developed. The porphyritic olivine crystals acquire with increasing stratigraphic height numerous randomly oriented amoeboidal and dendritic appendages or outgrowths that tend to obliterate the original olivine crystal shapes. These textures characterize the hopper stage (Fig. 5C). The hopper stage is by far predominant in this cycle extending over approximately 9 m thickness. Several minor inhomogeneities in the form of lumpy aggregates of porphyritic olivine are recognized in this cycle.

An approximately 10 cm thick layer of densely packed fine grained lensoid olivines, overlying the hopper olivine stage with an abrupt contact, is considered to represent the bottom of cycle 6 (from approximately 62.2 m to approximately 63.8 m). This cycle is outstanding due to its extreme thinness. The porphyritic stage is represented in this cycle by an approximately 5 cm thick layer of up to 1 mm diameter olivine crystals with rounded outlines in loose packing. The upper part of the porphyritic stage is characterized by the appearance of rod and horseshoe olivine that leads into an approximately 3 cm thick layer of mixed rod and horseshoe olivines. This transition zone is overlain by an approximately 140 cm thick layer of hopper olivine that is in turn overlain by lensoid olivine of the following cycle (cycle 7).

STRATIGRAPHY OF THE BRC ULTRAMAFIC ROCKS

Figures 6 and 7 depict the major stages of crystal habits within each identified igneous cycle in the western and the eastern cut. Barring large scale tectonic disruptions these figures probably represent stratigraphic columns since the BRC is a steeply dipping rock complex.

WESTERN CUT

The western cut is 160 m long; however, this is not the true thickness of the ultramafic unit, since both the northern and the southern extremities are covered with overburden. Thirteen cycles have been distinguished (Fig. 6). One of these (cycle 10) is a troctolite that has abrupt contacts to the overlying and underlying ultramafic units. Both its composition and the abrupt contact may indicate a tectonic emplacement. A part of cycle 12 is composed of subrounded fragments that are mainly of dunitic composition and range from grains to pebbles in size. Frequently they contain vaguely spherical chromite accumulations. A number of chromitite and pyrite fragments are also present. Preliminary outcrop investigations indicate that the chromitite fragments are part of a disrupted chromitite layer. The chromitite layer suites investigated by Scoates (1983) and Watson (1985) occur in cycle 13.

EASTERN CUT

The 200 m long eastern cut started approximately 20 m from the northern edge (stratigraphic bottom) of the ultramafic unit. A total of 13 cycles were distinguished in the cut. Parts of cycle 10 in the eastern cut are similar both in composition and texture to parts of cycle 12 in the western cut. It is at present unknown whether this distinctively disrupted and inhomogeneous rock layer containing rounded to subrounded fragments of chromitite, dunite and pyrite is continuous between the western and the eastern cut, i.e. a distance of approximately 700 m. This rock layer may coincide with Scoates' (1983) "disrupted layer suite".

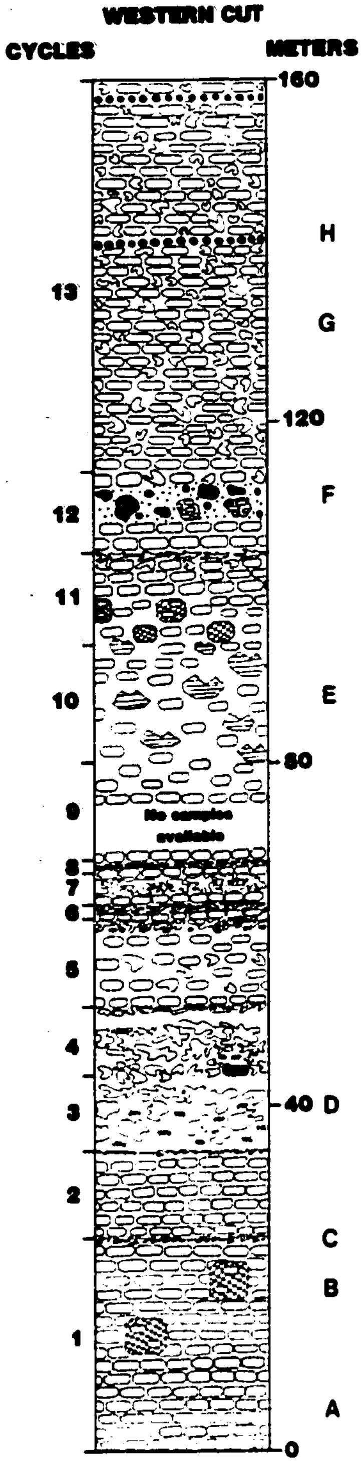

Figure 6: Western cut; schematic petrography and magmatic cycles. A. Lensoid stage olivine. B. Porphyritic stage olivine and clinopyroxene oikocrysts containing olivine inclusions. C. Thin layer of hopper stage olivine. D. Hopper stage olivine with abundant devitrified glass. E. Troctolite. F. Disrupted rock layer containing dunite, chromitite and pyrite fragments and spherical chromite accumulations. G. Rock layer including olivine of the following textural stages: Porphyritic, rods, rods with buds, and horseshoe. H. Chromitite layer.

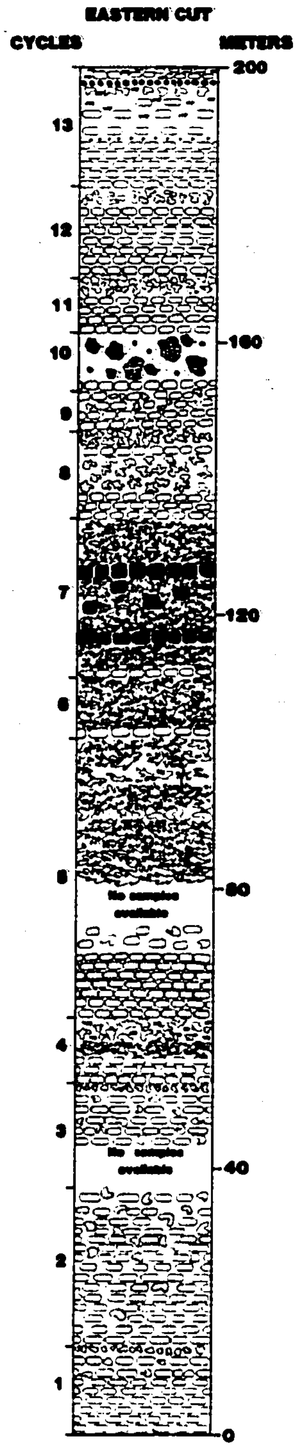

Figure 7: Eastern cut; schematic petrography and magmatic cycles. (See caption of Fig. 6 for explanation of symbols).

Although there are similarities between these two cuts such as: a) the number and approximate thickness of cycles; b) sequence of crystal habit development; c) occurrence of a disrupted rock layer; and d) the chromitite layers occurring in cycle 13 of the ultramafic sequence, there are also distinct differences such as: 1) The occurrence of a troctolite layer (cycle 10 western cut) and 2) distinct differences in the development and distribution of crystal habits. Cycles in the eastern cut are characterized by a predominance of hopper olivine at the expense of all other crystal stages, whereas western cut cycles are characterized by relatively thick basal lensoid stage and porphyritic stage olivine and an ample development of all intermediate crystal stages leading eventually to the hopper stage. Moreover, dendritic olivines have only been encountered in the eastern cut.

The significance of these differences are discussed in the concluding remarks.

PETROCHEMISTRY AND Pt - Pd DISTRIBUTION

Table 1 lists the major element chemistry of two rock samples from the eastern cut taken at 18 m and 51.8 m respectively. The samples are from the top of two different magmatic cycles and are made up of a network of interlocked hopper olivine. These rocks are thought to have undergone rapid crystallization and thus have experienced little differentiation. The chemistry of these samples is thus expected to closely resemble the parental magma.

Table 1: Major elements in weight per cent of two rock samples from the BRC

	BRC 18 m	BRC 51.8 m		BRC 18 m	BRC 51.8 m
SiO_2	39.20	39.50	CaO	3.81	3.21
TiO_2	0.15	0.17	Na_2O	0.01	0.01
Al_2O_3	5.98	6.26	K_2O	0.01	0.01
Fe_2O_3*	10.90	11.50	P_2O_5	0.11	0.11
MnO	0.16	0.15	L.O.I.	9.45	8.95
MgO	28.70	29.10	TOTAL	98.46	98.95

Analysis by Bondar-Clegg & Company Ltd.

* Total Fe

Figures 8, 9, 10, 11 and 12 show that each cycle is characterized by distinctive concentrations of S, Cu, Ni, Cr, Pt and Pd. Minor inconsistencies between cycle boundaries and chemistry are the result of 2 m sampling lengths used prior to the recognition of the magmatic cycles; in some places they overlap cycle boundaries.

Figures 8 and 9 show a close correlation between the concentrations of Pt, Pd, S, Cu and Ni in the western cut. Two discrete zones with high concentrations

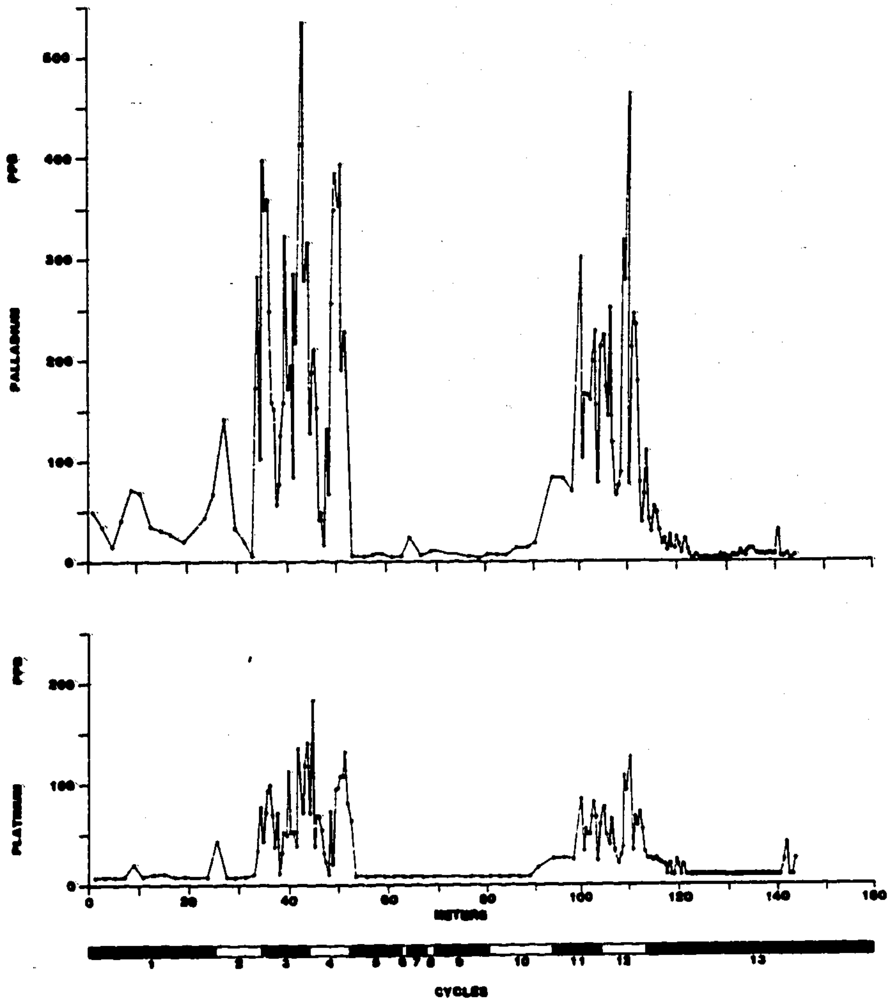

Figure 8: Western cut; concentrations of Pt and Pd versus distance from the base of the ultramafic unit. Location, number and thickness of magmatic cycles are indicated at the bottom of the diagram. (Hachured portion represents a sample gap).

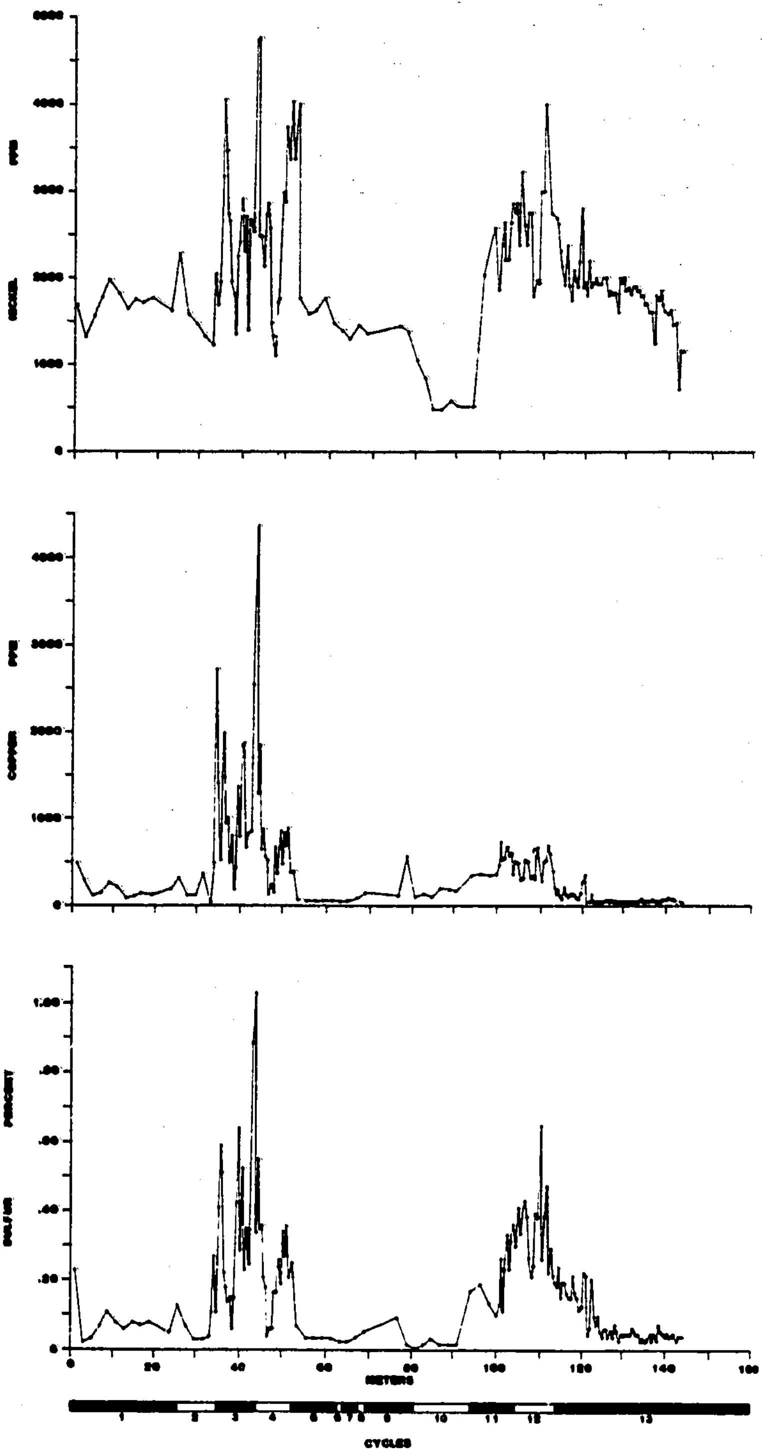

Figure 9: Western cut; concentrations of S, Cu and Ni. (For additional explanations, see caption of Fig. 8).

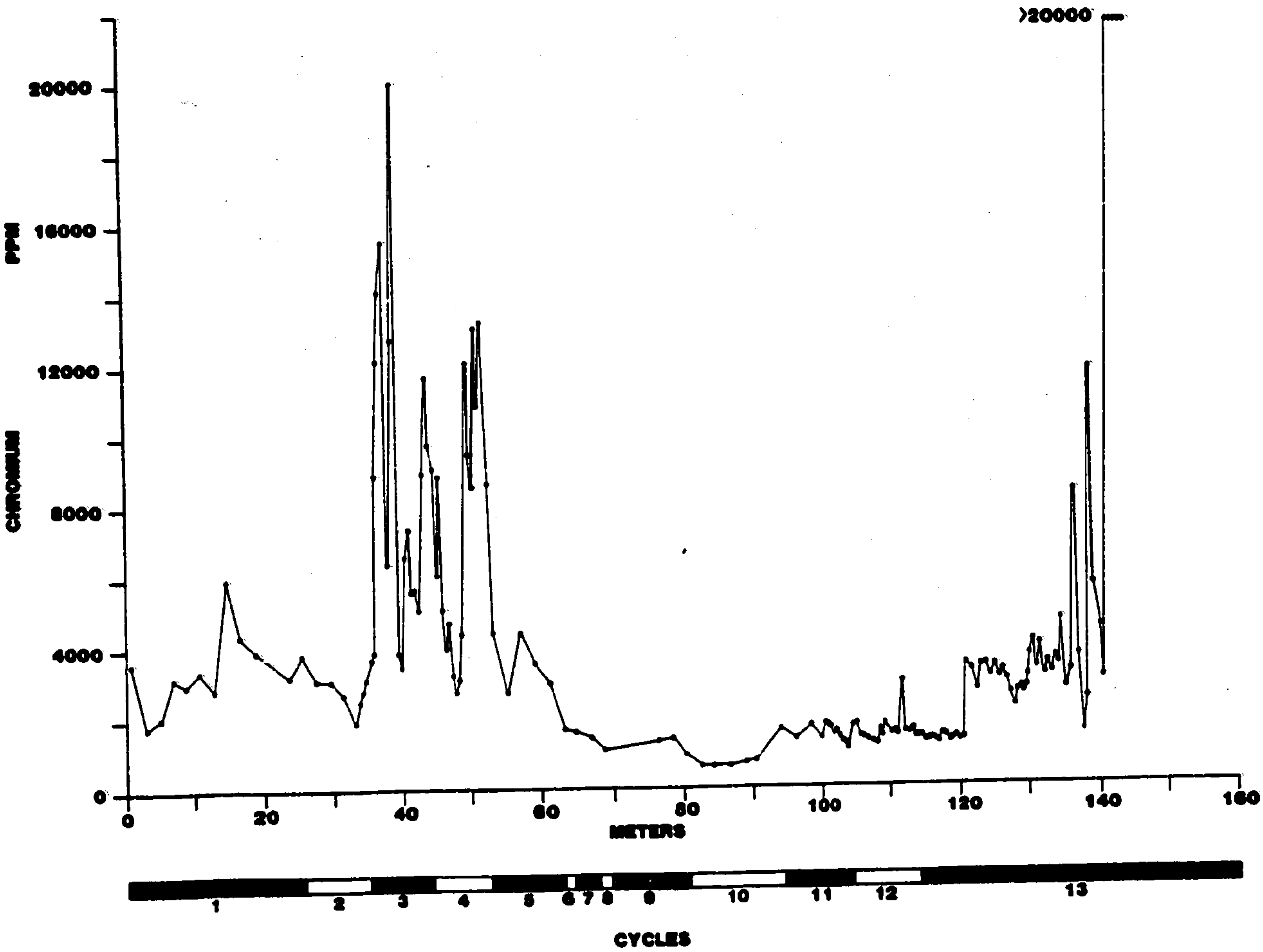

Figure 10. Western cut; concentration of Cr. (For additional explanation see caption of Fig. 8).

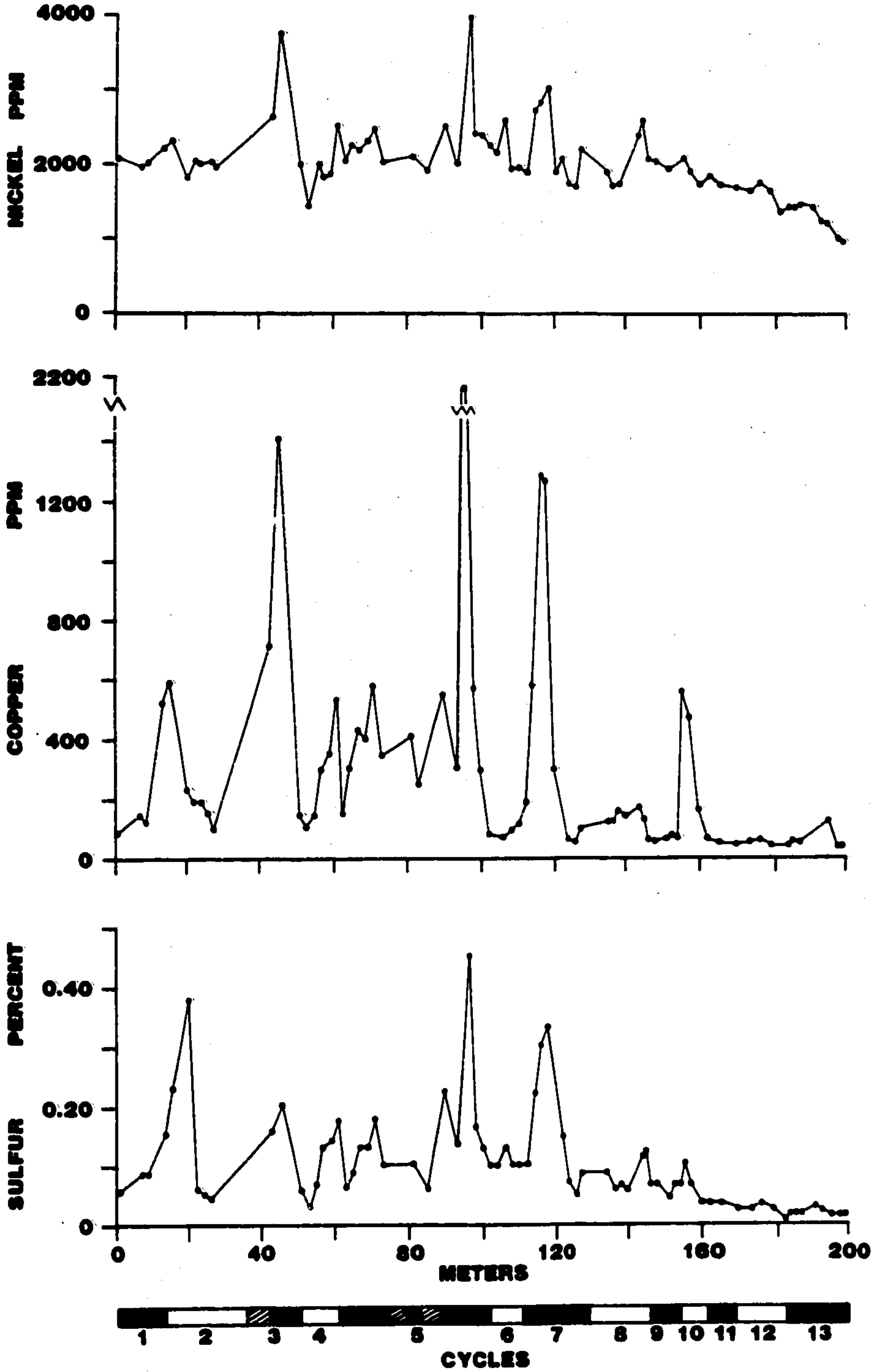

Figure 11. Eastern cut; concentrations of S, Cu and Ni. (For additional explanations, see caption of Fig. 8).

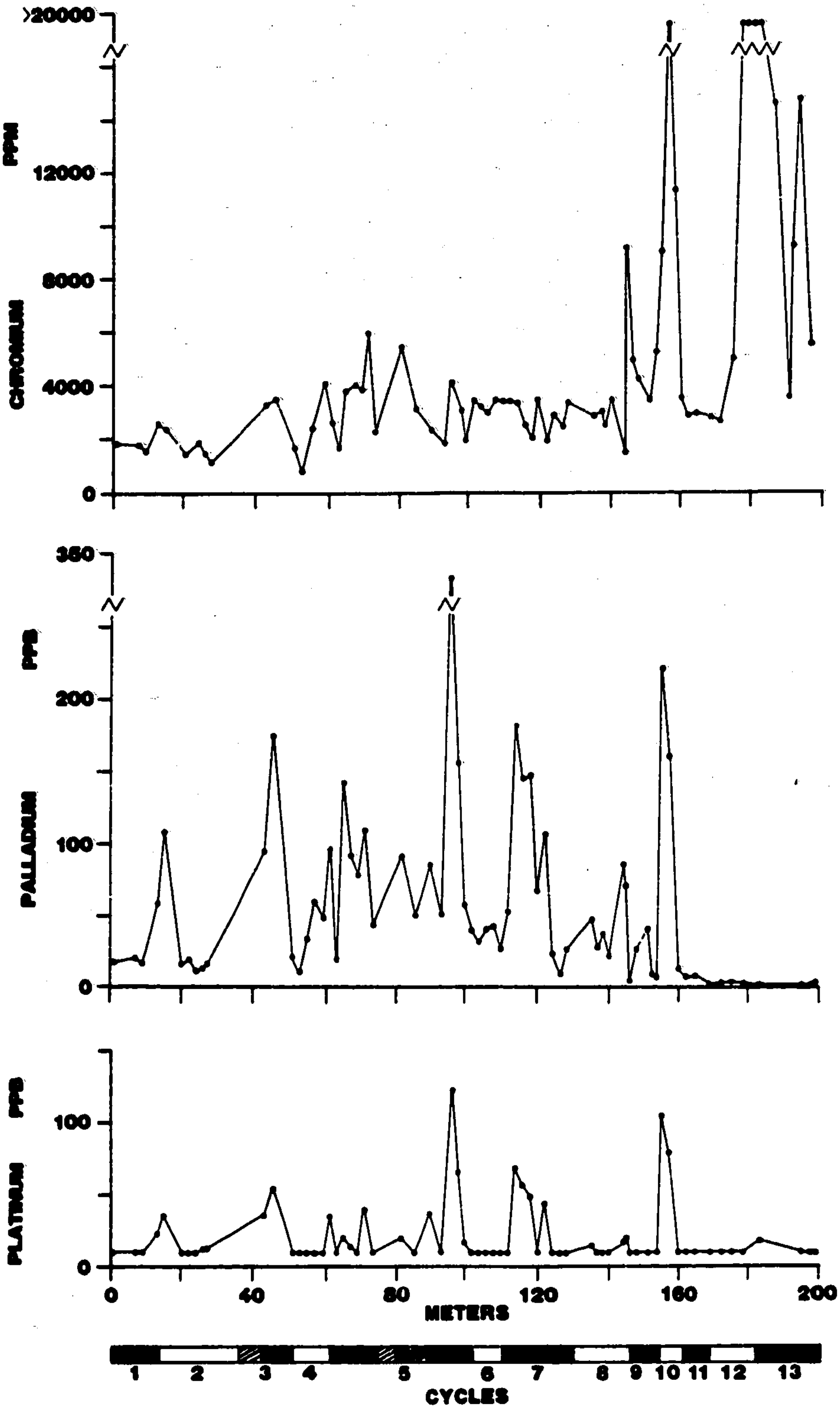

Figure 12: Eastern cut; concentrations of Pt, Pd and Cr. (For additional explanations, see captin of Fig. 8).

of these elements are recognized: a) coinciding with cycles 3 and 4; and b) roughly coinciding with cycles 11 and 12. Figure 10 shows the Cr concentrations in the western cut. Concentrations of Cr are found in cycles 3 and 4 and in the lower part of cycle 5, i.e. coinciding with some the cycles carrying high sulphides concentrations. This correlation, however is not repeated in cycles 11 and 12. The close correlation between concentrations of S and Ni indicates that most of the Ni - above a certain as yet undetermined base value - is bound in sulphide minerals. The progressive decline in Ni concentrations above cycle 12, however, is interpreted to be caused by a progressive differentiation of the parental magma. A similar effect is seen in the Ni contents of the eastern cut (Fig. 11) from cycle 6 up.

CHROMITE AS A PGE COLLECTOR IN THE BRC

Chromite is reported to be a good but erratic collector of PGE; for example, significant enrichment in Pt, Pd and Rh in chromitites of the Stillwater Complex has been reported by Crocket (1979), Page et al. (1976), and Page (1980). The association of PGE with chromitites of the UG - 2 and the Merensky Reefs are commented on by Hiemstra (1979). Recent investigations on chromite specimens of the BRC by Talkington et al. (1983) identified laurite (Ru, Os, Ir) S_2 and iridosmine (Os, Ir, Ru alloy) inclusions but no Pt and only negligible amounts of Pd were detected.

The role of chromite as a collector of Pt and Pd in the BRC is ambiguous. The good correlation of the Cr concentration with the other analyzed elements in cycles 3 and 4 of the western cut (Figs. 6, 7 and 8) reflects a coincidence in the concentrations of chromite and sulphides. Without any further investigations of these chromites for their contents of Pt and Pd it is impossible to state if and in what quantities Pt and Pd are associated with the chromites of these cycles. The lack of correlation between the concentrations of Cr, Pt and Pd of cycles 11 and 12 of the western cut (Figs. 6 and 8) indicates that in these cycles Pt and Pd are associated with sulphides only. However, in cycle 10 of the eastern cut the correlation of Cr, Pt and Pd and the absence of sulphides (Figs. 11 and 12) suggests that in this rock layer, Pt and Pd are associated with chromite. Chromite layers in the stratigraphically higher cycles 12 and 13 are, on the other hand, not associated with Pt and Pd as evidenced by the absence of a correlation between the concentrations of Pt, Pd and Cr in these cycles (Fig. 12).

CU/NI VS PT/PD

It is a well known observation that Ni strongly partitions into olivine whereas Cu tends to concentrate in the residual melt of differentiating ultramafic magma and that the ratio Cu/Ni is therefore a good indicator of the degree of differentiation of a magma. Naldrett and Cabri (1976) and Naldrett et al. (1982) suggested the existence of a negative correlation between the Cu/Ni ratio and the Pt/Pd ratio in sulphide-rich rocks of tholeiitic provenance and of low Pt/Pd and Cu/Ni ratios in sulphides associated with komatiitic rocks. However, Page et al. (1980) reported Pt/Pd ratios fluctuating with stratigraphic position and a positive correlation between Cu/Ni ratio and the Pt/Pd ratio of the Fiskenaesset complex of southern Greenland.

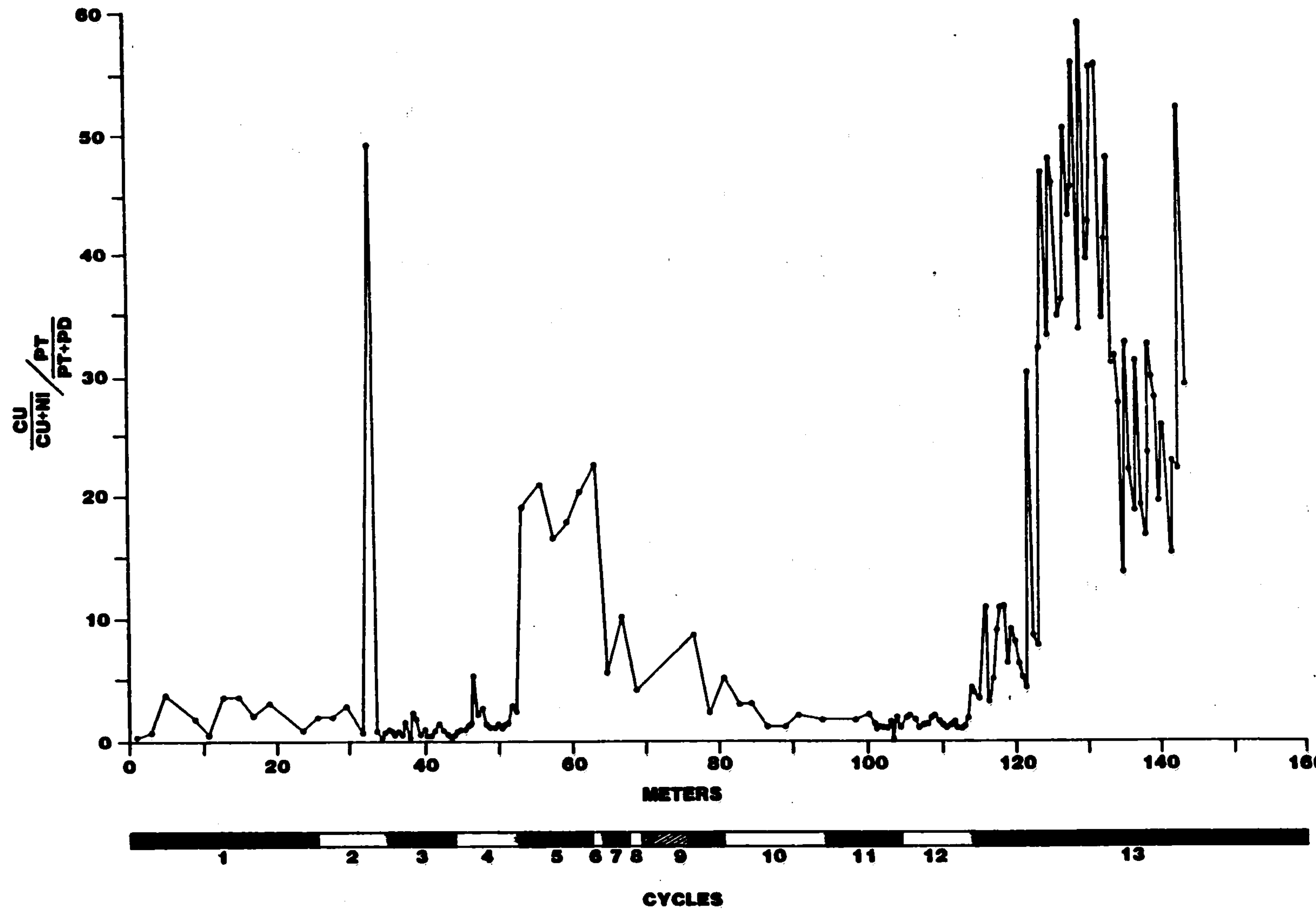

Figure 13: Western cut; ratio of Cu/(Cu + Ni) vs. Pt (Pt + Pd)

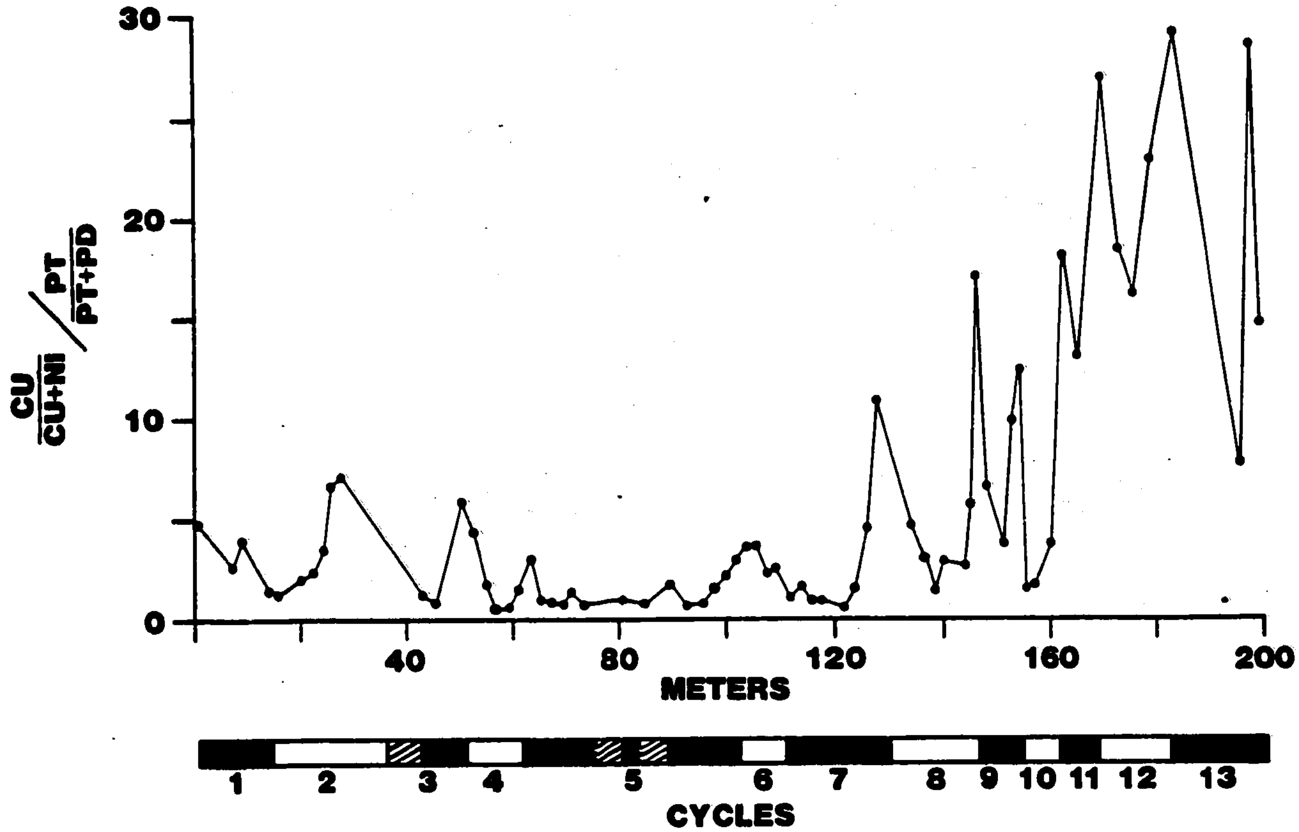

Figure 14: Eastern cut; ratio of Cu/(Cu + Ni) vs. Pt (Pt + Pd)

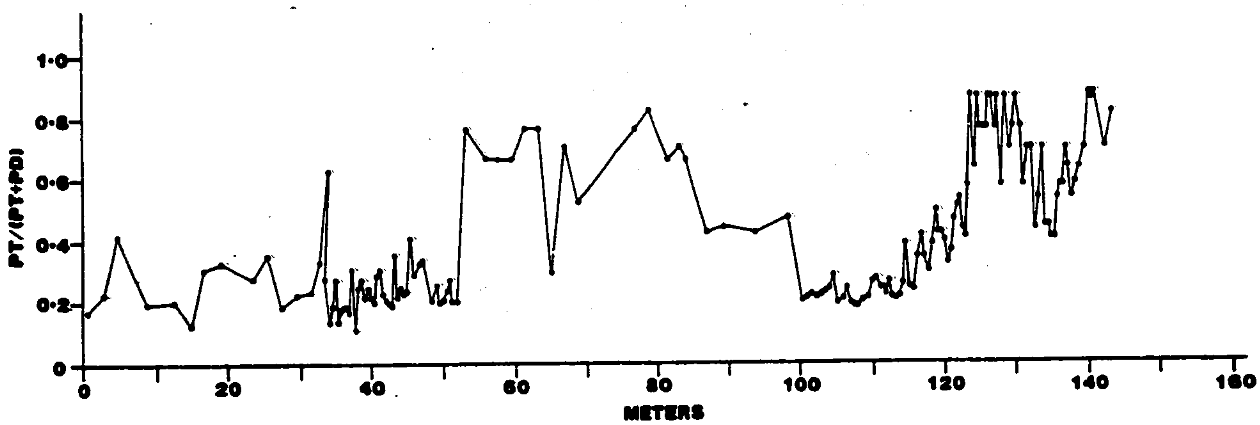

Figure 15: Western cut; ratio of Pt/(Pt + Pd)

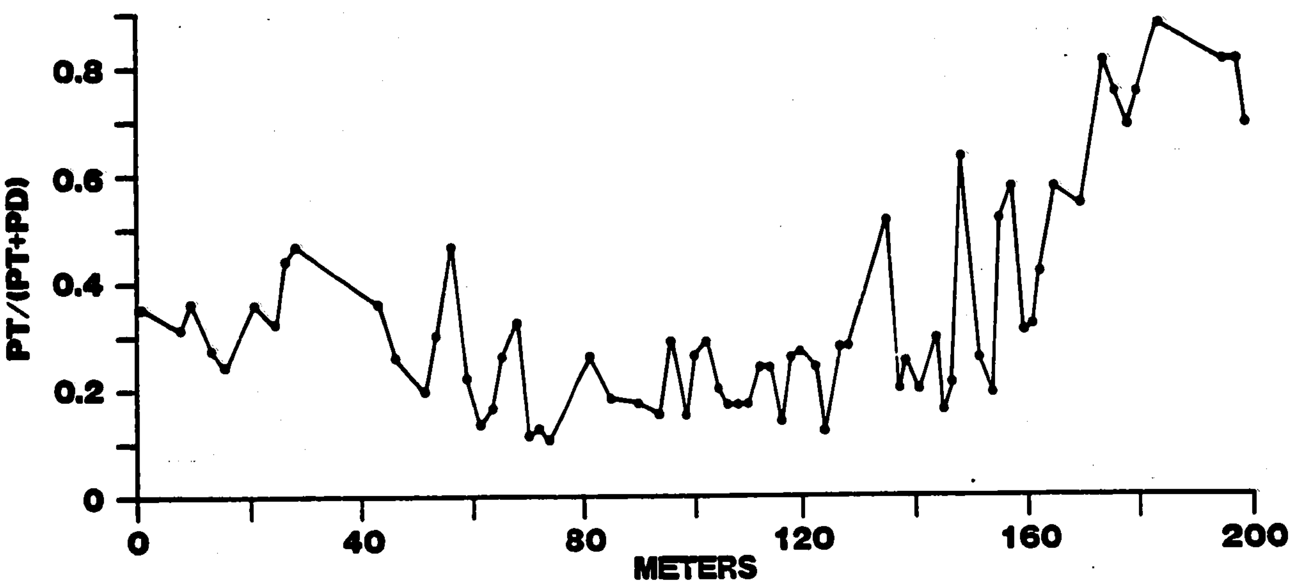

Figure 16: Eastern cut; ratio of Pt/(Pt + Pd)

The Cu/Ni vs Pt/Pd ratios of the western and the eastern cuts (Figs. 13, 14) show erratic fluctuations with a tendency to increase with stratigraphic height. Inspection of the Pt/Pd ratios (Figs. 15 and 16) shows only minor fluctuations and that much of the fluctuation in Figures 13 and 14 is due to a rise of the Cu/Ni ratio with increasing stratigraphic height that is primarily attributed to a concurrent increase in magmatic differentiation.

It is therefore concluded that in the BRC there appears to be no evidence of changes in the Pt/Pd ratio that can be directly attributed to magmatic differentiation.

CHONDRITE NORMALIZED PGE RATIOS

The ratios of PGE are supposed to be of use in characterizing the genesis and history of the parental magma (Naldrett et al., 1979 and 1982). Chondrite normalized PGE ratios (average chondrite concentrations, McBryde 1972) of several samples of the eastern cut and the mean of these samples are plotted on Figure 17. Two of these samples (48 m, 54 m) show a strong depletion in Pt and Pd, respectively. Average chondrite normalized PGE ratios from the Levack W and the Little Stobie mines published by Hoffman et al. (1979) are plotted for comparison. The ratios of the Sudbury sulphides and those of the BRC are comparable although the PGE concentrations in the BRC are much lower.

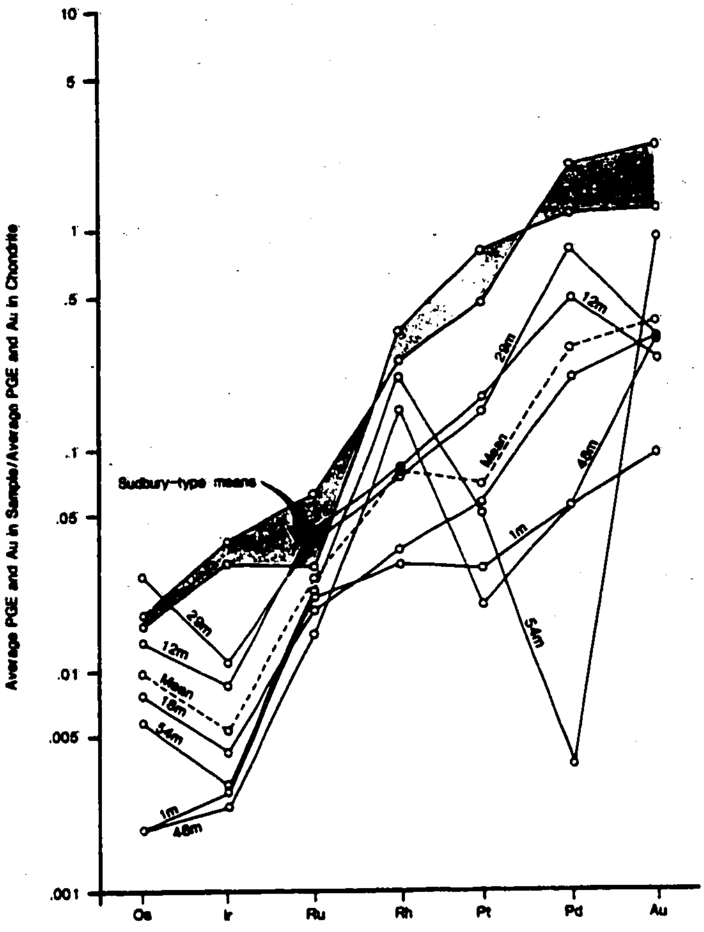

Figure 17: Chondrite normalized PGE contents of the BRC. Sudbury-type means plotted using data from the Levack W and the Little Stobie Mine (Hoffmann et al., 1979).

DISCUSSION

Sampling across most of the ultramafic unit of the BRC demonstrated the existence of discrete rock layers characterized by distinctive crystal habits and elevated concentrations of Pt and Pd. Maximum Pt and Pd concentrations recorded were 179 ppb Pt and 532 ppb Pd; however, higher concentrations (511 ppb Pt and 1145 ppb Pd) were detected in samples taken from the disrupted rock layer (part of cycle 12) approximately 50 m east of the western cut.

It was shown that the BRC exhibits cyclic units, defined by unidirectional successions of crystal habits. The crystal habits are dependent on the degree of supersaturation that is mainly a function of the melt's cooling rate. Supersaturation due to rapid loss of confining pressure and/or loss of volatiles (Lofgren and Donaldson, 1975; Donaldson, 1976) or due to inhomogeneous distribution of crystallization centres (Lofgren 1983) is discounted since these potential causes are expected to affect the magma mass equally throughout its entire thickness. The delineation of these cyclic units casts doubt on the previously held interpretations of the BRC as a single magmatic intrusion.

Experimental evidence (Donaldson, 1976, 1979) indicates that rapid cooling (at least up to 80°C per hour) is necessary to induce the type of skeletal olivine growth observed in the upper parts of the cyclic units in a magma of a composition similar to that of the ultramafic part of the BRC. Cooling rates of this magnitude are exceptional, but theoretically possible, in a magma chamber replenished with hot and dense fresh magma. Double diffusive convection concomitant with violent turbulence will ensue in the injected magma, if the resident magma and the injected magma are sufficiently different both in their temperatures and densities (Huppert and Sparks, 1980). However, no evidence of turbulence nor of substantial compositional differences between cycles have been observed. Moreover, it is difficult to envisage the physical configuration and the mechanics of a magma chamber that could accept repeated (at least thirteen) magma pulses that are then subjected to a comparable, relatively rapid cooling history.

An alternative model that envisages the BRC as an edifice of subaerial volcanic flows is tentatively proposed. The absence of additional evidence such as flow breccia, flow boundaries etc. detracts from this model; however, it appears much more readily to account for the repeated high cooling rates and the observed cyclical repetition of crystal habits. The behaviour of komatiitic flows has been studied recently by Huppert et al. (1984) and Huppert and Sparks (1985). They report that cooling rates as high as 1000°C per hour can be readily accommodated in these flows. High cooling rates such as these lead to large delays in the nucleation of olivine (Donaldson, 1979). It could be speculated that olivine crystallization may have been delayed until cessation of turbulence in the magma, accounting for the observed undisturbed crystal layering. However, much more field and laboratory work is required before the true nature of this complex is recognized.

It is suggested that other ultramafic bodies should be investigated for cyclical igneous units regardless of their presumed geological nature and Cr mineralization in order to determine their PGE potential. Emphasis should be placed on sampling any sulphide-bearing units present.

EXPLORATION FOR PGE IN THE BRC

PGE in the BRC appear to be concentrated in discrete rock layers characterized by anomalous, laterally fluctuating mineralization. Anomalous amounts of Pt and Pd in the western cut are essentially restricted to igneous cycles 3, 4, 11 and 12 (Fig. 8) whereas Pt and Pd in rocks of the eastern cut show a diffuse distribution pattern of several rather lower peaks of concentration in several igneous cycles (Fig. 12).

Although superficially similar, it appears to be impossible to correlate the rock units of the western with those of the eastern cut. The only truly common feature - discounting the chemical composition and certain described petrographic details - appears to be the occurrence of chromitite layers in the stratigraphically higher layers of the ultramafic unit. However, the Pt and Pd distribution patterns show some features that could be used in their exploration:

a) the chromitite-rich stratigraphically higher layers appear to be devoid of Pt and Pd. (An exception is cycle 10 of the eastern cut which contains high Cr, Pt and Pd mineralization).

b) generally low concentrations of Pt and Pd within the stratigraphically low parts of the ultramafic units.

c) good and consistent correlation of Pt, Pd and sulphides.

Exploration for PGE in the ultramafic portion of the BRC should therefore concentrate on those rock layers that are located stratigraphically below the chromitite layers and contain sulphides. Identification of these rock layers outside of the Chrome exposure, which are generally covered by overburden and disrupted by faulting, may be facilitated by the use of a gradiometer. This instrument was shown by Watson (1982) to be successful in the identification of individual chromitite layers in the Chrome exposure. The results of this trial may justify the expectation of similarly useful results in areas covered with overburden.

ACKNOWLEDGEMENTS

The author wishes to acknowledge the support received from the Manitoba Department of Energy and Mines in the course of this work. It is my pleasure to acknowledge the contribution of the many student assistants involved in the cutting program, especially R. Gaba. B. Schmidtke diligently and cheerfully drafted the figures; P. Gilbert and C. McGregor provided petrographical and mineralogical assistance. D. Berk and his crew assisted both in the field and laboratory work. Special thanks go to Drs. W. D. McRitchie, M. A. F. Fedikow and G. H. Gale for their encouragement and assistance in various aspects of the fieldwork and manuscript preparation.

REFERENCES

Bannatyne, B. B., and Trueman, D. L.
1982: Chromite reserves and geology of the Bird River Sill, Manitoba; Manitoba Mineral Resources Division, Open File Report, 82-1.

Bateman, J. D.
1943: Bird River chromite deposits, Manitoba; Transactions, Canadian Institute of Mining and Metallurgy, v. 46, p. 154-183.

Coats, C. J. A., Stockford, H. R. and Buchan, R.
1979: Geology of the Maskwa West nickel deposit; Canadian Mineralogist, v. 17, p. 309-318.

Colony, R. J.
1920: A norite of the Sudbury type in Manitoba; Canadian Mining Journal, v. 41,p. 967-970.

Cooke, H. C.
1922: Geology and mineral resources of the Rice Lake and Oiseau River areas, Manitoba; Geological Survey of Canada, Summary Report, 1921, pt. c, 36 p.

Crocket, J. H.
1979: Platinum-group elements in mafic and ultramafic rocks: A survey; Canadian Mineralogist, v. 17, p. 391-402

Davies, J. F.
1952: Geology of the Oiseau (Bird) River Area, Manitoba; Manitoba Mines Branch, Publication 51-3.

Donaldson, C. H.
1974: Olivine crystal types in harrisitic rocks of the Rhum pluton and Archean spinifex rocks; Geological Society of America Bulletin, v. 85, p. 1721-1726.

1976: An experimental investigation of olivine morphology; Contributions to Mineralogy and Petrology, v. 57, p. 187-213.

1979: An experimental investigation of the delay in nucleation of olivine in mafic magmas; Contributions to Mineralogy and Petrology, v. 69, p. 21-32.

Drever, H. I., and Johnston, R.
1957: Crystal growth of forsteritic olivine in magmas and melt; Transactions, Royal Society, Edinburgh, v. 63, pt. 2, no. 13.

Ermanovics, I. F., and Froese, E.
1978: Metamorphism of the Superior Province in Manitoba, in Metamorphism of the Canadian Shield; Geological Survey of Canada, Paper 78-10, p. 17-24.

Haffty, J., Riley, L. B., and Goss, W. D.
1977: A manual on fire assaying and determination of the noble metals in geologic materials; United States Geological Survey, Bulletin 1445.

Hiemstra, S. A.
1979: The role of collectors in the formation of the platinum deposits in the Bushveld complex; Canadian Mineralogist, v. 17, p. 469-482.

Hoffmann, E. L., Naldrett, A. J., Alcock, R. A. and Hancock, R. G. V.
1979: Comparison of the noble metal content of the Levack West mine and the Little Stobie mine, Ontario, Canada; Canadian Mineralogist, v. 17, p. 437-451

Hoffmann, E. L., Naldrett, A. J., Van Loon, J. C., Hancock, R. G. V., and Manson, A.
1978: The determination of all the platinum - group elements and gold in rocks and ore by neutron activation analysis after preconcentration by a nickel sulphide fire-assay technique on large samples; Analytica Chimica Acta, v. 102, p. 157-176.

Huppert, H.E. and Sparks, R.S.J.
1980: The fluid dynamics of a basaltic magma chamber replenished by influx of hot, dense ultrabasic magma; Contributions to Mineralogy and Petrology, v. 75, p. 279-289.

1985: Komatiites I: Eruption and flow; Journal of Petrology, v. 26, p. 694-725.

Huppert, H.E., Sparks, R.S.J., Turner, J.S., and Arndt, N.T.
1984: The emplacement and cooling of komatiite lavas; Nature, v. 309, p. 19-23.

Lofgren, G. E.
1983: Effect of heterogeneous nucleation on basaltic textures: A dynamic crystallisation study; Petrology, v. 24, pt. 3, p. 229-255.

Lofgren, G. E. and Donaldson, C. H.
1975: Curved branching crystals and differentiation in comb-layered rocks; Contributions to Mineralogy and Petrology, v. 58, p. 309-319.

Martin, R. F., and MacLean, W. H.
1973: Crystal growth forms in Hawaiitic lavas of Heimay, Iceland [abs.]; Geological Society of America, 1973 Annual Meeting, v. 5, no. 7, p. 726-727.

McBryde, W. A. E.
1972: Platinum metals; in: Encyclopedia of geochemical and environmental sciences 1972; ed., R.W. Fairbridge; Van Nostrand Reinhold Co., New York.

Naldrett, A. J., and Cabri, L. J.
1976: Ultramafic and related mafic rocks: Their classification and genesis with special reference to the concentration of nickel sulphides and platinum group elements; Economic Geology, v. 71, p. 1131-1158.

Naldrett, A. J., Hoffmann, E. L., Green, A. H., Chen-Lin, Chou, Naldrett, S.R., and Alcock, R.A.
1979: The composition of Ni-sulphide ores, with particular reference to their content of PGE and Au; Canadian Mineralogist, v. 17, p. 403-415.

Naldrett, A. J., Innes, D. G., Sowa, J., and Gorton, M. P.
1982: Compositional variations within and between five Sudbury ore deposits; Economic Geology, v. 77, p. 1519-1534.

Osborne, T. C.
1949: Petrography and petrogenesis of the Bird River Chromite bearing sill; Unpublished M. Sc. thesis, University of Manitoba, 66 p.

Page, N. J., Myers, J. S., Haffty, J., Simon, F.O., and Aruscavage, P. J.
1980: Platinum, Palladium, and Rhodium in the Fiskenaesset complex, Southwestern Greenland; Economic Geology, v. 75, p. 907-915.

Page, N. J., Rowe, J. J. and Haffty, J.
1976: Platinum metals in the Stillwater Complex, Montana; Economic Geology, v.71, p. 1352-1363.

Scoates, R. F. J.
1983: A preliminary stratigraphic examination of the ultramafic zone of the Bird River Sill, southeastern Manitoba; in Manitoba Mineral Resources Division, Report of Field Activities, 1983, p. 70-83.

Springer, G. D.
1948: Geology of the Cat Lake - Maskwa Lake area; Manitoba Mines Branch, Preliminary Report, 48-7.

1949: Geology and mineral deposits of a part of southeastern Manitoba; Precambrian, v. 22, n. 8.

1950: Mineral deposits of the Cat Lake - Winnipeg River area; Manitoba Mines Branch, Publication 49-7.

Talkington, W., Watkinson, D. H., Whittaker, P. J. and Jones, P. C.
1983: Platinum-Group-Minerals inclusions in chromite from the Bird River Sill, Manitoba; Mineralium Deposita, v. 18, p. 245-255.

Timmins, E. A., Turek, A., and Symons, D. T. A.
1985: U-Pb zircon geochronology and paleomagnetism of the Bird River greenstone belt, Manitoba, [abs.]; Geological Association of Canada/Mineralogical Association of Canada, Annual meeting 1985.

Trueman, D. L.
1971: Petrological, structural and magnetic studies of a layered basic intrusion, Bird River Sill, Manitoba; Unpublished M. Sc. thesis, University of Manitoba, 67 p.

1980: Stratigraphy, structure and metamorphic petrology of the Archean greenstone belt at Bird River, Manitoba; Unpublished Ph. D. thesis, University of Manitoba, 151 p.

Watson, D.M.
1982: Chromite Resources of the Bird River Area, in Manitoba Mineral Resources Division, Report of Field Activities, 1982, p. 60-63.

1985: Chromite reserves of the Bird River Sill; Manitoba Energy and Mines, Open File Report, OF85-8.

Wright, J. F.
1932: Geology and mineral deposits of part of southeastern Manitoba; Geological Survey of Canada, Memoir 169, 150 p.

APPENDIX 1. Western Cut (2 m interval samples) Rock Geochemical Data

Sample #	From	To (m)	(1) Mg %	(2) S %	(3) Cu ppm	(4) Ni ppm	(5) Pt ppb	(6) Pd ppb	(7) Au ppb	(8) Cr ppm	(9) Fe %
1	0	2	14.2	0.23	487	1788	10	50	2	3650	9.21
2	2	4	13.2	0.02	288	1323	10	34	2	1780	9.11
3	4	6	13.8	0.03	116	1555	10	14	2	2100	9.24
4	6	8	15.7	0.07	145	1775	10	40	3	3230	9.65
5	8	10	16.1	0.11	257	1979	19	72	5	3030	8.96
6	10	12	16.2	0.08	211	1825	10	69	5	3390	8.95
7	12	14	16.9	0.06	83	1692	15	34	2	2880	8.35
8	14	16	17.3	0.08	101	1856	15	30	2	5960	8.94
9	16	18	17.4	0.07	140	1718	10	26	3	4340	8.83
10	18	20.6	17.3	0.08	129	1767	10	18	63	3960	8.39
11	22.6	24.6	16.8	0.05	192	1621	10	43	5	3240	9.10
12	24.6	26.6	16.2	0.13	327	2385	41	140	10	3900	9.28
13	26.6	28.6	16.0	0.07	116	1570	10	32	5	3150	9.01
14	28.6	30.1	15.6	0.03	119	1477	10	19	2	3130	9.09
15	30.3	32.3	14.2	0.03	365	1322	10	26	5	2750	8.90
16	32.3	34.3	14.5	0.08	946	1683	39	84	8	2750	10.50
17	34.3	36.3	13.9	0.40	1109	2467	96	343	16	8850	9.94
18	36.3	38.3	13.4	0.13	920	1717	39	111	8	11250	9.27
19	38.3	40.3	14.2	0.31	1448	2419	49	213	16	7850	9.62
20	40.3	42.3	14.9	0.42	1141	2551	55	255	15	4860	9.88
21	42.3	44.3	13.2	0.69	1953	2951	92	364	29	11590	10.70
22	44.3	46.3	14.6	0.26	689	2313	52	166	8	5980	8.91
23	46.3	48.3	15.1	0.06	286	1315	22	37	8	2970	8.31
24	48.3	50.3	15.1	0.24	719	2708	82	290	22	8560	9.08
25	50.3	52.3	16.0	0.19	604	2717	99	291	24	10720	9.55
26	52.3	54.3	17.4	0.06	54	1770	10	4	4	4430	9.14
27	54.3	56.3	17.1	0.03	49	1588	10	3	2	2800	8.91
28	56.3	58.3	16.6	0.03	49	1627	10	5	2	4250	8.65
29	58.3	60.3	17.5	0.03	51	1771	10	5	2	3660	8.98
30	60.3	62.3	16.5	0.03	47	1478	10	3	2	2560	8.79
31	62.3	64.3	14.8	0.02	40	1398	10	3	2	1730	7.91
32	64.3	65.7	15.6	0.02	49	1453	10	23	2	1660	7.93
33	65.9	67.9	14.5	0.03	79	1353	10	4	2	1570	8.41
34	67.9	69.7	13.7	0.05	135	1446	10	9	2	1170	10.50
35	75.6	77.6	15.1	0.09	107	1363	10	3	2	1340	8.08
36	77.6	79.6	12.7	0.01	542	1158	10	2	5	1490	7.72
37	79.6	81.6	10.1	0.00	93	853	10	5	2	914	7.69
38	81.6	83.6	6.99	0.01	116	493	10	4	2	495	5.96
39	83.6	85.6	7.61	0.02	97	481	10	5	2	505	6.75
40	85.6	87.6	7.01	0.01	185	575	10	13	62	510	6.47
41	87.6	89.6	7.00	0.01	168	496	10	12	6	597	5.66
42	89.6	91.3	7.24	0.01	159	495	16	17	2	648	5.96
43	93.7	94.4	14.2	0.16	327	2089	24	84	4	1670	9.11

Sample #	From	To (m) (1)	(2) Mg %	(3) S %	(4) Cu ppm	(5) Ni ppm	(6) Pt ppb	(7) Pd ppb	(8) Au ppb	(9) Cr ppm	(10) Fe %
44	95.4	97.4	14.2	0.19	349	2099	25	84	6	1380	8.32
45	97.4	99.4	17.1	0.13	328	1858	23	70	6	17101	8.11
46	99.4	101.4	16.9	0.14	541	1930	46	163	12	1590	8.65
47	101.4	103.4	17.1	0.18	556	2042	44	135	11	1720	8.20
48	103.4	105.4	18.0	0.29	411	2214	27	109	9	1480	8.86
49	105.4	107.4	17.9	0.29	337	2214	33	152	10	1840	9.59
50	107.4	109.4	18.6	0.26	447	2090	26	109	9	1600	9.22
51	109.4	111.7	18.6	0.38	543	2406	51	203	11	1730	10.60

Notes:

(1) The chemistry of each sample represents the composition of approximately 2m thickness of the Bird River Sill; variations from this norm are introduced by outcrop configuration.

(2) Analyses by Manitoba Energy and Mines, Chemical Laboratory; borate fusion - atomic absorption (Minimum sensitivity 0.1%).

(3) Analyses by Manitoba Energy and Mines, Chemical Laboratory; Leco Furnace (Minimum sensitivity 0.01%).

(4) Analyses by Manitoba Energy adn Mines, Chemical Laboratory; borate fusion - atomic absorption (Minimum sensitivity 5 ppm).

(5) Analyses by Manitoba Energy and Mines, Chemical Laboratory; borate fusion - atomic absorption (Minimum sensitivity 10 ppm).

(6) Analyses by Bondar-Clegg & Company Ltd.; Aqua regia-fire assay-DC plasma (Minimum sensitivity 10 ppb).

(7) Analyses by Bondar-Clegg & Company Ltd.; Aqua regia-fire assay-DC plasma (Minimum sensitivity 2 ppb).

(8) Analyses by Bondar-Clegg & Company Ltd.; Aqua regia-fire assay-DC plasma (Minimum sensitivity 2 ppb).

(9) Analyses by Bondar-Clegg & Company Ltd.; borate fusion-DC plasma (Minimum sensitivity 1 ppm).

(10) Analyses by Bondar-Clegg & Company Ltd.; borate fusion-DC plasma (Minimum sensitivity 0.01%).

Conventions:

15 ppb Pt were assigned the value of 7 ppb Pt
2 ppb Au were assigned the value of 1 ppb Au

APPENDIX 2. Western Cut (50 cm interval samples) Rock geochemical data

Sample	Sample interval From	To	(1) (2) Mg %	(3) S %	(4) Cu ppm	(5) Ni ppm	(6) Pt ppb	(7) Pd ppb	(8) Au ppb
100	32.3	32.8	15.40	0.04	16	1225	15	4	1856
101	32.8	33.3	16.00	0.11	490	2048	30	172	2536
102	33.3	33.8	17.00	0.27	2720	1679	73	272	2837
103	33.8	34.3	15.60	0.11	1407	1949	40	102	3160
104	34.3	34.8	17.20	0.41	527	3165	69	400	3755
105	34.8	35.3	17.80	0.59	1460	4070	89	348	3951
106	35.3	35.8	14.80	0.51	1971	3470	96	358	8860
107	35.8	36.3	14.60	0.22	936	2735	66	247	12100
108	36.3	36.8	14.40	0.18	997	2515	34	157	14080
109	36.8	37.3	14.00	0.14	482	1953	68	150	15488
110	37.3	37.8	15.00	0.15	791	1803	15	56	6373
111	37.8	38.3	14.60	0.06	165	1346	27	77	12782
112	38.3	38.8	14.60	0.15	421	2345	48	123	19987
113	38.8	39.3	16.80	0.42	1354	2410	46	156	3906
114	39.3	39.8	16.80	0.64	978	2905	109	322	3518
115	39.8	40.3	14.60	0.29	1835	2305	49	170	6576
116	40.3	40.8	15.00	0.52	1847	2705	49	194	7358
117	40.8	41.3	16.80	0.23	656	1400	35	85	5516
118	41.3	41.8	16.80	0.35	803	2660	132	286	5637
119	41.8	42.3	14.80	0.25	842	2535	68	216	5048
120	42.3	42.8	12.80	0.89	2530	4730	114	414	8972
121	42.8	43.3	9.60	1.03	4440	4750	137	532	11693
122	43.3	43.8	13.20	0.34	1267	2485	68	277	9746
123	43.8	44.3	14.80	0.55	1533	2475	179	317	9031
124	44.3	44.8	15.20	0.35	623	2130	34	117	6033
125	44.8	45.3	15.40	0.36	855	2515	65	188	8800
126	45.3	45.8	15.40	0.21	545	2725	64	210	5050
127	45.8	46.3	16.80	0.18	507	2565	50	152	4019
128	46.3	46.8	14.40	0.04	121	1473	28	40	4695
129	46.8	47.3	14.40	0.06	204	1322	20	48	3274
130	47.3	47.8	16.00	0.06	155	1096	15	14	2771
131	47.8	48.3	16.80	0.14	568	1711	70	131	3108
132	48.3	48.8	16.00	0.14	365	1743	18	67	4155
133	48.8	49.3	15.60	0.26	859	2980	92	256	12573
134	49.3	49.8	15.40	0.19	483	2875	93	350	9437
135	49.8	50.3	15.60	0.34	831	3750	104	387	8310
136	50.3	50.8	16.00	0.27	689	3375	104	354	13090
137	50.8	51.3	16.20	0.36	890	4625	126	395	11890
138	51.3	51.8	17.20	0.21	379	3375	78	191	13210
139	51.8	52.3	18.60	0.24	389	4000	61	228	8492
140	99.4	100.0	18.00	0.10	345	3375	81	301	1162
141	100.0	100.5	18.80	0.13	455	2375	30	104	1369

Sample	Sample interval From	To	(1) Mg %	(2) S %	(3) Cu ppm	(4) Ni ppm	(5) Pt ppb	(6) Pd ppb	(7) Au ppb (8)
142	100.5	101.0	16.80	0.26	713	2625	50	165	1833
143	101.0	101.5	19.00	0.11	507	2200	46	164	1730
144	101.5	102.0	18.00	0.23	545	2200	47	160	1696
145	102.0	102.5	18.80	0.33	657	2625	63	199	1496
146	102.5	103.0	18.00	0.23	576	2875	78	228	1578
147	103.0	103.5	18.80	0.31	595	2750	63	155	1392
148	103.5	104.0	19.20	0.36	352	2875	20	79	1280
149	104.0	104.5	19.60	0.30	495	2400	56	213	1216
150	104.5	105.0	19.20	0.41	481	3250	73	223	1113
151	105.0	105.5	20.00	0.31	284	2625	45	174	1759
152	105.5	106.0	18.40	0.32	302	2400	35	145	1790
153	106.0	106.5	17.20	0.43	518	2750	60	251	1429
154	106.5	107.0	19.00	0.38	499	2750	31	117	1387
155	107.0	107.5	18.40	0.26	315	1795	18	65	1328
156	107.5	108.0	18.40	0.21	339	1983	27	74	1220
157	108.0	108.5	18.80	0.24	299	1954	34	88	1193
158	108.5	109.0	18.80	0.39	551	3000	104	317	1607
159	109.0	109.5	18.80	0.38	661	3000	90	278	1419
160	109.5	110.0	18.80	0.65	917	4125	123	461	1781
161	110.0	110.5	20.00	0.26	279	1820	20	87	1533
162	110.5	111.0	19.60	0.38	496	2750	64	211	1547
163	111.0	111.7	20.00	0.47	520	2750	55	244	1444
164	111.7	112.0	17.80	0.22	691	2700	67	243	2937
165	112.0	112.5	18.40	0.29	588	2625	51	178	1556
166	112.5	113.0	20.00	0.21	389	2375	28	79	1538
167	113.0	113.5	20.40	0.19	210	2125	25	39	1643
168	113.5	114.0	24.00	0.18	130	1925	22	66	1377
169	114.0	114.5	20.40	0.23	178	2400	34	108	1415
170	114.5	115.0	18.00	0.15	98	1900	22	41	1411
171	115.0	115.5	21.00	0.19	70	1750	20	28	1267
172	115.5	116.0	22.40	0.19	210	2100	23	54	1316
173	116.0	116.5	20.00	0.16	129	2000	21	49	1375
174	116.5	117.0	19.60	0.15	86	1900	19	30	1334
175	117.0	117.5	20.80	0.15	110	2200	17	16	1227
176	117.5	118.0	20.80	0.21	115	2800	16	21	1299
177	118.0	118.5	21.20	0.16	140	1900	15	9	1270
178	118.5	119.0	20.40	0.15	90	1950	17	25	1233
179	119.0	119.5	19.60	0.11	78	1800	15	14	1248
180	119.5	120.0	19.60	0.12	137	2200	15	12	1307
181	120.0	120.5	21.00	0.22	267	2600	21	22	1233
182	120.5	121.0	21.40	0.21	335	2500	16	15	1244
183	121.0	121.5	22.00	0.04	33	1825	15	6	3506
184	121.5	122.0	22.40	0.06	44	1800	16	20	3299
185	122.0	122.5	23.20	0.20	122	2200	15	10	1572
186	122.5	123.0	20.00	0.09	35	1900	15	5	2677
187	123.0	123.5	20.80	0.07	37	1950	15	2	3434

Sample	Sample interval From	To (1)	(2) Mg %	(3) S %	(4) Cu ppm	(5) Ni ppm	(6) Pt ppb	(7) Pd ppb	(8) Au ppb
188	123.5	124.0	21.20	0.09	38	1950	15	4	3476
189	124.0	124.5	20.80	0.05	37	2000	15	2	3162
190	124.5	125.0	22.00	0.03	33	1925	15	2	3437
191	125.0	125.5	20.80	0.06	44	1925	15	2	3134
192	125.5	126.0	22.80	0.06	44	2000	15	2	3258
193	126.0	126.5	22.60	0.03	35	2000	15	2	3056
194	126.5	127.0	20.00	0.05	37	1800	15	2	2545
195	127.0	127.5	21.60	0.03	32	1850	15	2	2163
196	127.5	128.0	20.80	0.07	29	1825	15	2	2693
197	128.0	128.5	22.00	0.05	32	1825	15	5	2786
198	128.5	129.0	18.80	0.02	24	1600	15	2	2663
199	129.0	129.5	23.20	0.04	36	2000	15	3	2397
200	129.5	130.0	23.60	0.04	36	1950	15	2	3197
201	130.0	130.5	24.00	0.04	32	2000	15	2	3744
202	130.5	131.0	22.00	0.04	26	1850	15	2	4135
203	131.0	131.5	21.20	0.04	32	1875	15	5	3367
204	131.5	132.0	20.80	0.06	31	1800	15	3	4042
205	132.0	132.5	22.40	0.05	28	1900	15	3	3166
206	132.5	133.0	21.60	0.04	27	1900	15	9	3538
207	133.0	133.5	22.80	0.04	32	1850	15	6	3217
208	133.5	134.0	22.80	0.02	48	1850	15	3	3688
209	134.0	134.5	21.40	0.03	63	1800	15	8	3439
210	134.5	135.0	21.60	0.02	26	1800	15	8	4613
211	135.0	135.5	22.80	0.02	32	1700	15	10	2728
212	135.5	135.8	21.20	0.03	38	1700	15	10	3297
213	136.0	136.5	18.40	0.04	28	1600	15	6	8358
214	136.5	137.0	21.20	0.02	50	1600	15	5	3687
215	137.0	137.5	15.20	0.04	45	1250	15	5	1458
216	137.5	138.0	24.00	0.02	55	1800	15	3	2432
217	138.0	138.5	22.80	0.07	38	1750	15	4	11560
218	138.5	139.0	23.80	0.05	36	1850	15	6	5660
219	139.0	139.5	21.60	0.04	52	1700	15	5	4393
220	139.5	140.0	21.20	0.03	41	1625	15	4	4279
221	140.0	140.5	20.80	0.04	54	1600	15	39	4517
222	140.5	141.0	20.80	0.03	76	1650	15	3	3117
223	141.0	141.5	18.00	0.03	58	1450	15	2	20,000
224	141.5	142.0	18.40	0.04	60	1500	36	6	20,000
225	158.0	158.5	10.40	0.02	12	700	15	2	20,000
226	158.5	159.0	15.20	0.03	28	1150	15	3	20,000
227	159.0	159.5	14.60	0.03	20	1150	16	4	20,000

Notes:

(1) The chemistry of each sample represents the composition of approximately 0.5 m thickness of the Bird River Sill; variations from this norm are introduced by outcrop configuration.

(2) Analyses by Bondar-Clegg & Company Ltd.; multiple acid digestion-atomic absorption. (Minimum sensitivity 0.01%).

(3) Analyses by Bondar-Clegg & Company Ltd.; gravimetry. (Minimum sensitivity 0.01%).

(4) Analyses by Bondar-Clegg & Company Ltd.; multiple acid digestion-atomic absorption. (Minimum sensitivity 1 ppm).

(5) Analyses by Bondar-Clegg & Company Ltd.; multiple acid digestion-atomic absorption. (Minimum sensitivity 2 ppm).

(6) Analyses by Bondar-Clegg & Company Ltd.; multiple acid digestion-atomic absorption. (Minimum sensitivity 15 ppb).

(7) Analyses by Bondar-Clegg & Company Ltd.; multiple acid digestion-atomic absorption. (Minimum sensitivity 2 ppb).

(8) Analyses by Bondar-Clegg & Company Ltd.; borate fusion-DC plasma. (Minimum sensitivity 1 ppm).

Conventions:

15 ppb Pt were assigned the value of 7 ppb Pt
2 ppb Pd were assigned the value of 1 ppb Pd

APPENDIX 3. Eastern Cut (2 m interval samples) Rock Geochemical Data

Sample #	From	To (m) (1)	(2) Mg %	(3) S %	(4) Cu ppm	(5) Ni ppm	(6) Pt ppb	(7) Pd ppb	(8) Au ppb	(9) Cr ppm
1	0	1.1	18.75	0.06	88	2081	10	18	5	1834
2	6	8.1	17.50	0.09	150	1950	10	21	39	1790
3	8.1	10.2	14.80	0.08	124	2008	10	17	4	1514
4	12.0	14.9	17.00	0.16	538	2240	23	59	10	2580
5	14.9	15.6	15.00	0.23	598	2335	36	108	11	2370
6	19.1	21.1	14.50	0.38	237	1827	10	17	439	1450
7	21.1	23.1	14.00	0.06	186	2043	10	20	6	1859
8	23.1	25.1	16.80	0.05	186	1999	10	12	6	n.d.
9	25.1	27.1	17.50	0.04	156	2015	13	14	3	1465
10	27.1	28.1	18.80	0.04	108	1951	10	17	2	1130
11	42.0	44.5	19.00	0.16	735	2635	36	95	10	3555
12	45.2	46.1	17.75	0.20	1400	3748	44	176	13	3730
13	50.0	52.0	17.00	0.06	159	1984	10	22	8	1634
14	52.0	54.0	13.90	0.03	113	1454	10	11	3	780
15	54.0	56.0	12.40	0.07	157	1999	10	34	7	2150
16	56.0	58.0	17.00	0.13	300	1810	10	60	7	4090
17	58.0	60.0	17.10	0.14	363	1865	10	49	13	2639
18	60.0	62.0	21.00	0.18	540	2505	35	97	7	n.d.
19	62.0	64.0	19.70	0.06	147	2035	10	20	6	1636
20	64.0	66.0	20.00	0.09	310	2260	20	143	13	3790
21	66.0	68.0	19.50	0.13	439	2195	14	92	15	4020
22	68.0	70.0	20.00	0.13	408	2300	10	79	11	3850
23	70.0	72.0	19.10	0.18	580	2485	40	110	10	5493
24	72.0	74.6	19.00	0.10	346	2010	10	44	9	2240
25	80.2	82.2	18.50	0.10	417	2060	20	92	7	5484
26	82.2	83.7	17.30	0.06	253	1898	10	51	5	3060
27	88.7	90.7	16.00	0.22	559	2575	37	86	16	2282
28	92.7	94.9	17.75	0.14	328	2010	10	52	9	1760
29	95.4	97.0	20.00	0.45	2160	3995	123	337	43	4101
30	97	99	20.00	0.17	590	2420	66	157	21	3030
31	99	101	20.00	0.13	298	2395	17	58	11	1909
32	101	103	21.00	0.10	93	7305	10	40	7	3390
33	103	105	20.00	0.10	84	2115	10	32	5	3215
34	105	107	20.00	0.13	81	2620	10	41	6	2960
35	107	109	18.00	0.10	100	1918	10	27	4	3434
36	106	111	18.00	0.10	128	1962	10	27	4	3330
37	111	113	17.80	0.10	191	1886	10	53	7	3330
38	113	115	17.80	0.22	586	2770	69	183	11	3270
39	115	117	16.40	0.30	1290	2845	57	146	33	2445
40	117	119	14.30	0.33	1260	3075	49	148	24	1970
41	119	121	13.50	0.10	290	1897	10	68	8	3432
42	121	123	13.70	0.15	508	2063	44	107	9	1850
43	123	125	16.10	0.07	70	1781	10	24	6	2883

Sample #	From	To (m) (1)	(2) Mg %	(3) S %	(4) Cu ppm	(5) Ni ppm	(6) Pt ppb	(7) Pd ppb	(8) Au ppb	(9) Cr ppm
44	125	127	14.70	0.05	56	1724	10	9	2	2390
45	127.4	136	17.90	0.09	107	2204	10	37	3	3297
46	136	137.6	17.50	0.06	99	1831	10	28	4	2780
47	137.6	138.8	18.00	0.07	154	1722	10	38	3	2906
48	138.8	141.3	20.00	0.06	123	1776	10	22	4	2430
49	143.8	144.7	19.25	0.11	160	2375	17	86	3	3419
50	144.7	145.2	17.75	0.12	100	2480	20	71	2	1481
51	145.2	146.8	18.00	0.07	60	2065	10	5	2	9115
52	146.8	149.4	20.00	0.07	49	2015	10	27	3	4820
53	149.4	151.9	19.20	0.05	58	1902	10	41	2	4232
54	151.9	153.4	21.20	0.07	77	2058	10	9	2	3360
55	153.4	154.5	20.00	0.07	67	1917	10	7	3	5194
56	154.5	156.1	18.50	0.10	560	2092	105	222	6	8940
57	156.1	158.1	14.50	0.07	460	1882	79	161	5	5.04% (10)
58	158.1	161.4	17.00	0.04	140	1717	10	13	2	11250
59	161.4	163.0	19.20	0.04	61	1803	10	7	4	3471
60	163.0	167.2	18.80	0.04	52	1705	10	8	4	2750
61	167.2	171.1	19.40	0.03	46	1689	10	2	2	2803
62	171.1	173.8	15.80	0.03	57	1617	10	3	4	2700
63	173.8	176.9	18.60	0.04	61	1706	10	4	3	2552
64	176.9	180.4	18.00	0.03	46	1599	10	3	9	4900
65	180.4	182.1	15.80	0.01	52	1319				6.20% (10)
66	182.1	184.2	18.50	0.02	47	1396	18	2	2	20000
67	184.2	186.3	15.50	0.02	66	1386	n.d.	n.d.	n.d.	5.80% (10)
68	186.3	188.7	13.80	0.02	55	1424	n.d.	n.d.	n.d.	20000
69	190.0	192.0	16.40	0.04	25	1381	n.d.	n.d.	n.d.	1.54% (10)
70	192.0	194.0	19.00	0.03	29	1254	n.d.	n.d.	n.d.	3430
71	195.0	196.0	16.50	0.02	124	1207	10	2	3	9137
72	197.5	198.5	16.20	0.02	30	995	10	2	3	14680
73	198.5	199.5	15.80	0.02	37	937	10	4	7	5392

Notes:

(1) The chemistry of each sample represents the composition of approximately 2 m thickness of the Bird River Sill; variations from this norm are introduced by outcrop configuration.

(2) Analyses by Bondar-Clegg & Company Ltd.; multiple acid digestion-atomic absorption. (Minimum sensitivity 0.01%).

(3) Analyses by Manitoba Energy and Mines, Chemical Laboratory; Leco Furnace. (Minimum sensitivity 0.01%).

(4) Analyses by Manitoba Energy and Mines, Chemical Laboratory; Aqua Regia-atomic absorption. (Minimum sensitivity 5 ppm).

(5) Analyses by Bondar-Clegg & Company Ltd.; multiple acid digestion-atomic absorption. (Minimum sensitivity 2 ppm).

(6) Analyses by Bondar-Clegg & Company Ltd.; Aqua Regia-fire assay-DC plasma. (Minimum sensitivity 10 ppb).

(7) Analyses by Bondar-Clegg & Company Ltd.; Aqua Regia-fire assay-DC plasma. (Minimum sensitivity 2 ppb).

(8) Analyses by Bondar-Clegg & Company Ltd.; Aqua Regia-fire assay-DC plasma. (Minimum sensitivity 2 ppb).

(9) Analyses by Bondar-Clegg & Company Ltd.; borate fusion-DC plasma. (Minimum sensitivity 1 ppm).

(10) Analyses by Bondar-Clegg & Company Ltd.; sodium hydroxide fusion-atomic absorption. (Minimum sensitivity 0.01%).

Conventions:

10 ppb Pt were assigned the value of 5 ppb Pt
2 ppb Pd were assigned the value of 1 ppb Pd
2 ppb Au were assigned the value of 1 ppb Au